Published by :
http://www.ijert.org

International Journal of Engineering Research & Technology (IJERT)
ISSN: 2278-0181
Vol. 6 Issue 03, March-2017

Effect of TiO_2 Film Thickness Synthesized by Pulse Spray Pyrolysis Technique on the Response to UV- Illumination

M. Obaida, I. Moussa, S. A. Hassan, S. E. Demian and H. H. Afify
Solid State Physics Department,
National Research Centre, 33 El Bohouth St. (former El Tahrir St.),
Dokki, Giza, Egypt, P.O. 12622.

***Abstract*— Titanium Oxide films are deposited by pulse spray pyrolysis (PSP) technique on glass substrates. Samples with different thicknesses are prepared by keeping the substrate temperature constant at 400ºC while varying the spray time (30 - 90 min.). The crystal structure and phase are determined by GAXRD. Dislocation density is deduced from calculation of grain size obtained from the GAXRD. The energy gap, refractive index, film thickness and porosity are calculated from the transmittance spectra by adopting Swanepoel method. The photoconductivity of the samples is calculated by measuring the current before and after UV- illumination at constant voltage. The dynamic response to UV of the samples is obtained, with varying their thicknesses corresponding to On/ Off cycles of UV lamp. The prepared samples may be have an energy gap which is empty from inter-band states as inferred from the sharp absorption edge in the transmittance spectra and sharp decay of photocurrent in the dynamic response to UV illumination.**

Keywords*— Pulsed spray pyrolysis (PSP); thin film; titania anatase phase; UV- sensor; dynamic photoresponse.

I. INTRODUCTION

TiO_2 is considered one of the interesting and promising materials in the field of gas and photo sensors [1-6]. TiO_2 is widely used in a variety of applications such as paints, cosmetics, foodstuff and commonly used as an insulator in the electronic industry, in virtue of its versatile properties such as high refractive index, wide band gap of 3.2 eV and its high resistive ability for chemical and physical impacts [7, 8] . TiO_2 can be in one of three different crystal structures rutile, anatase and brookite. The former two structures which are most common belong to the tetragonal crystal system while brookite belongs to the orthorhombic system. The anatase phase shows the highest photocatalytic activity among the other two phases because of its considerably large energy gap [9, 10].

Synthesis of high performance titania UV- sensor films with good structural integrity is an important aspect in the design of high-efficiency UV- sensor reactors, ozone layer observation, plume detection of the skyrockets and environmental purity control [11-16]. TiO_2 in the form of thin film has been prepared by several methods such as sputtering, spray pyrolysis, sol-gel, pulsed laser deposition, chemical vapor deposition …etc [2,17-21].

The present study is intended to peruse the sensitivity of nanocrystalline TiO_2, with varying film thicknesses, to UV radiation prepared by low cost technique. The samples are prepared by pulse spray pyrolysis technique (PSP) from Tetratitanium isopropoxide (TTIP). Spray time at constant substrate temperature is manipulated provided that the deposited films have good adherence and homogenity. Structural, optical and electrical properties are tested. Our main study is focused on the samples sensitivity to UV illumination. Static response at variable dc bias voltage and dynamic response, (On/ Off) to UV lamp input-power, at constant bias voltage is investigated.

II. EXPERIMENTAL

Titanium oxide (TiO_2) films are prepared by pulsed spray pyrolysis (PSP) technique [21], since it is a simple, low cost and could be used for industrial scale they existed in the anatase phase only. PSP system with (On/ off- mode) keeps the substrate temperature to a great extent constant which improve the film / substrate adhesion, and allows enough time for film growth. The spray parameters: nozzle / substrate distance, flow rate of carrier gas (dry air), molarity of materials, spray pulse frequency, and substrate temperature are varied one at a time and are adjusted for values, until we obtain best adherence, homogeneous and pin hole free films. The system works automatically after feeding it with the optimum values [21]. Titanium isopropoxide or TTIP (Ti $\{OCH(CH_3)_2\}_4$) is used as a precursor dissolved in a solution of methyl alcohol and acetylacetonate (AcAc) as an attempt to excavate the effect of the solvent on the prepared films, although the common solvent reported in most publications is ethanol with acids [22-25]. TTIP is mixed with AcAc and stirred for 30 minutes to obtain a homogenous chelating solution. Afterwards methyl alcohol is added to the previously prepared solution and stirred for 1 h. The prepared spray solution with molarity 0.2 M is sprayed on ultrasonically pre-cleaned glass substrates at nozzle-substrate surface distance of 30 cm and substrate temperature 400ºC. The spray time is varied from 30 to 90 minutes while the air pump pulse frequency is set at 1 sec. On / 5 sec. Off- mode. Each run is repeated to ensure the reproducibility of the apparent feature of the deposited film.

Grazing angle X-ray diffraction equipment (GAXRD - Diano corroboration-USA equipment with Cu K_α radiation of λ= 1.514 Å) is used to elucidate the nature of samples structure, phase identifications and crystallite size. Double beam spectrophotometer (JASCO- 670 UV – VIS – NIR) with

International Journal of Engineering Research & Technology (IJERT)
ISSN: 2278-0181
Vol. 6 Issue 03, March-2017

wavelength range from 0.2 to 2.5 µm is used to measure transmittance and reflectance spectra. The photocurrent effect due to UV light is measured at room temperature with a setup which consists of UV-lamp (λ= 254 nm, power of 5 mW/cm^2), computerized interface multimeter (BK precession- Test Bench 390 A) and dc- power supply designed for such measurements.

III. RESULTS AND DISCUSSION

A. Structural Analysis

XRD patterns of TiO_2 films deposited on glass substrates at 400ºC for different spray times (30- 90 min.) are shown in Fig. 1. The deposited films show peak reflections (101), (004), (200), (105), (211), (204), (116), (220) and (215) which reflect the polycrystalline nature of the deposited films. It is found that the peaks are compatible with those listed in the standard card, (JCPDS No. #21-1272). It is observed that the height and number of the peaks increases progressively in sequence as the film thickness increases. The intensity of the peaks has the same sequence as those given in the reference file No. #21-1272.The peak position has no observable shift with increasing film thickness. The XRD patterns of the investigated samples are totally empty from any peaks related to any impurity or any other TiO_2 phases. This indicates that the prepared films are the pure Anatase phase with tetragonal crystalline structure and have strong preferred orientation along the (101) direction. It is clear that, with increasing spray time of the deposited TiO_2 films the characteristic peaks' intensity of the anatase phase is progressively strengthened which reflects the amelioration of both film crystallinity and grain size.

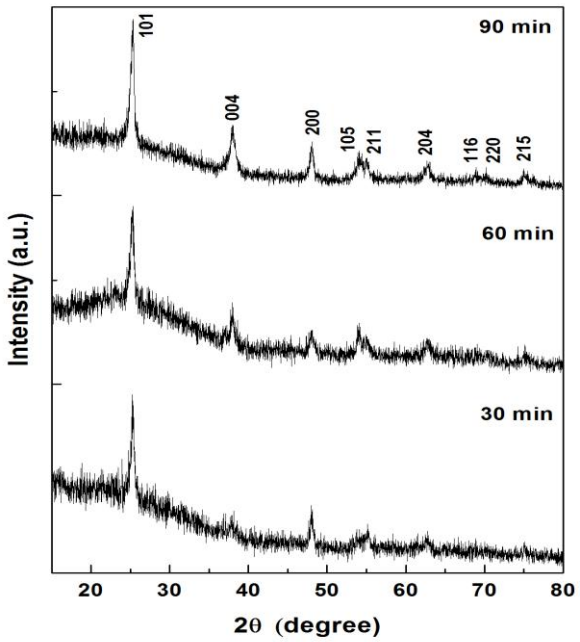

Fig. 1 XRD patterns of TiO_2 thin films deposited at 400ºC different spray times (film thickness).

B. Crystallite Size And Internal Strain

Crystallite size and lattice strain are calculated for samples which show more than one XRD peak by using Williamson-Hall relation in Eq. (1) [26]:

$$\frac{\beta_C \cos\theta}{\lambda} = \frac{1}{D} + \varepsilon\left(\frac{\sin\theta}{\lambda}\right) \quad (1)$$

Where, λ (1.5406Å) is the wave length of X-rays, β_c is the full width at half maximum (FWHM) in radian, ε is micro strain, D is grain size and θ is the diffraction angle (degree). The slope of the plot ($\beta_c \cos\theta/\lambda$) versus ($\sin\theta/\lambda$) gives the value of micro strain (ε) and the reciprocal of intercept on y-axis gives the grain size (D) value. Dislocation density δ is calculated using the approach Williamson and Smallmann relation in Eq. (2) [27]. The calculated values for both ε &D are given in Table 1.

$$\delta = 1/D^2 \quad (2)$$

- TABLE 1: THICKNESS, CRYSTALLITE SIZE, DISLOCATION DENSITY, STRAIN AND ENERGY GAP VALUES OF TiO_2 THIN FILM FOR DIFFERENT SPRAY TIMES.

Spray time (min.)	Parameters				
	Thickness (nm)	Crystallite size (D) (nm)	Dislocation density $(1/D^2)$ $(nm)^{-2}$	Strain (%)	Band gap (eV)
30	110	30.6	0.0011	0. 60	3.65
45	150	35.5	0.0008	0. 50	3.55
60	165	41.5	0.0006	0. 42	3.35
70	167	43.3	0.0005	0. 40	3.35
90	194	45.1	0.00049	0. 40	3.35

C. OPTICAL PROPERTIES

The transmittance (T) and reflectance (R) spectra of the investigated samples, deposited at constant substrate temperature 400ºC and different spray time, ranging from 30 to 90 min. are shown in Fig.2.

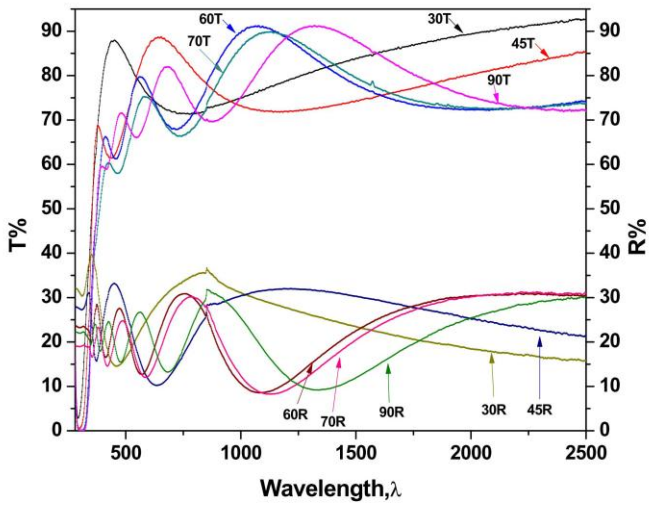

Fig. 2 Transmission spectra of TiO_2 thin films prepared at constant deposition temperature (400ºC) and different spray

International Journal of Engineering Research & Technology (IJERT)
ISSN: 2278-0181
Vol. 6 Issue 03, March-2017

These spectra are characterized by two salient features, sharp absorption edge and interference fringes regardless the spray time. However, films show high transmittance >85% which slightly decrease with increasing the film thickness.

The Envelope method, adopted by Swanepoel method is used [28], to calculate the film thickness for the deposited samples from the transmission spectra give in Fig.2. The obtained values are shown Table 1. Refractive index of the investigated samples is calculated by using the equations given by Swanepoel method [28]. The obtained value is found to be 2.03 in the wavelength range 0.6 to 2.5 µm. It is clear that the change in film thickness has no observable change on the refractive index.

The band gap energy (E_g) is estimated by using Tauc's equation (eq.3) [29] which represents the relationship between the incident photon energy (hν) and the absorption coefficient (α):

$$(\alpha h\upsilon) = A(h\nu - E_g)^n \quad (3)$$

Where A is a constant, E_g is the energy gap, hν is the photon energy and n is a constant, (2 or ½), for either indirect and direct allowed transition respectively. The plot representing $(\alpha h\nu)^2$ vs. (hν) which is related to the direct energy gap is shown in Fig.3. The straight line portion is extrapolated to intersect the x axis at (αhν) =0.The intersection point gives the energy gap.

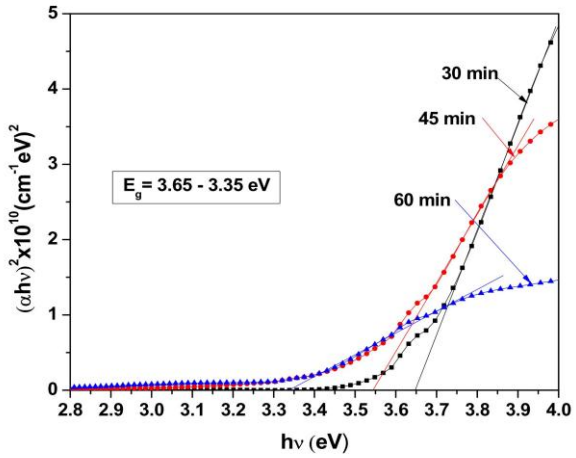

Fig. 3 Variation of $(\alpha h\nu)^2$ with photon energy for TiO_2 films prepared at different spray times.

The calculated values ranged from 3.35 to 3.65 eV, the energy gap decreases with increasing spray time. The samples deposited at short spray time (30 & 45 min.) have larger band gap energy (3.65 eV) while those deposited at longer spray time (60, 70 and 90 min.) have the same smaller band gap energy (3.35 eV). This is likely due to quantum size effect, accompanied with the decreased crystallite size which is in the nanometer scale.

The porosity (P) is determined using the Lorenz-Lorentz relation (eq.4) [30]:

$$P(\%) = 1 - \frac{n^2 - 1}{n^2 + 2} \cdot \frac{n_b^2 + 2}{n_b^2 - 1} * 100 \quad (4)$$

Where n_b is the refractive index of the pore-free anatase TiO_2 (n_b = 2.4918) [30] and n is the refractive index of the thin films. The calculated value of porosity using the above equation (by substituting the calculated value of sample refractive index) is found to be 19%.

D. ELECTRICAL MEASUREMENTS

The deposited pure TiO_2 films on glass substrates have a high resistance ranging from 50 MΩ to 60 MΩ as measured by Keithly electrometer. This makes it a suitable candidate for use as a good insulating material in many electronic applications. This high resistance is probably attributed to the presence of adsorbed oxygen. These states allow adsorption of oxygen molecules at the TiO_2 film surface or at the grain boundaries which extracts electrons giving rise to an increase in the film resistivity. Since, the investigated samples are prepared in no vacuum setup and the carrier gas is air, so, the obtained films have great probability to adsorb oxygen. Therefore, the investigated samples give higher resistance >50 MΩ/ 3mm.

The I-V measurements at room temperature (RT) for as-deposited TiO_2 films deposited at 60, 70 and 90 minutes under the UV illumination of λ= 254 nm with power of 5mW/cm^2 and different applied DC voltage are plotted in Fig 4.The incident photons energy from the used lamp is 4.88 eV which is greater than the energy gap of the tested samples 3.65 eV. As a result electron-hole pair generation is proceeded producing excess free carriers. At certain applied bias voltage these generated carriers are collected by the electrodes inducing the measured photocurrent. The photocurrent shows nearly linear relation with the applied voltage as shown in

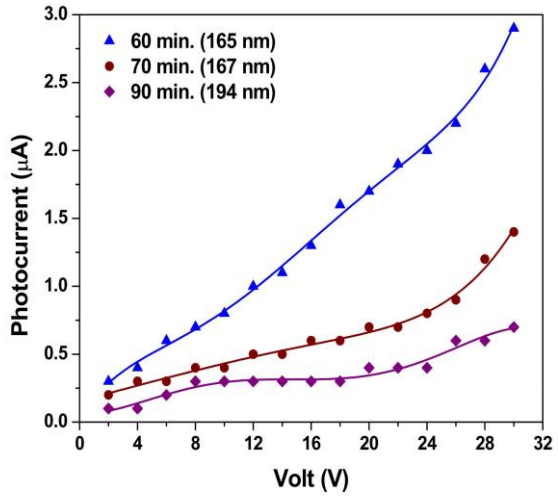

Fig. 4 I-V characteristics measurements with different spray time (film thickness) of TiO_2 layers.

International Journal of Engineering Research & Technology (IJERT)
ISSN: 2278-0181
Vol. 6 Issue 03, March-2017

It is worth to note that the sample deposited at 60 min. spray time, thinner film, has the greater photocurrent than the other samples thicker films, deposited at 70 & 90 minutes. This unexpected result may be due to the probable existence of recombination centers such as imperfections and presence of existing impurities which are in their lower level in thinner than thicker samples. The samples deposited at 30 and 45 minutes have no response to the UV- light. This could be attributed to both lower film thickness and the high adsorption of oxygen on the film surface.

The effect of changing the incident UV intensity on the photocurrent at constant applied voltage (30 volt) is demonstrated in Fig.5. It is obvious that at the short distance (1 cm) between the UV lamp and the sample surface all sample, normally show the higher values of the photocurrent, which decreases to its lower value at the longer distance. This could be explained by the change in UV intensity according to the basic inverse square law [$1\alpha\ 1/x^2$].

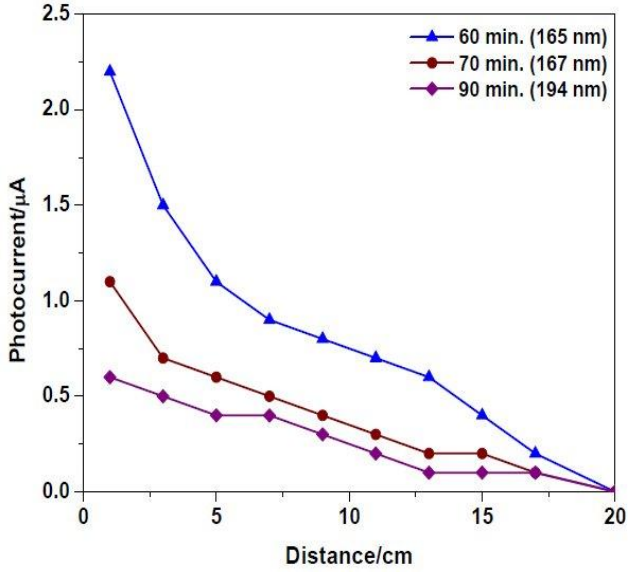

Fig. 5. The effect of distance on the photocurrent intensity of TiO_2 samples at 30 Volts.

The dynamic response is performed on TiO_2 film samples deposited at 60 minutes, which give highest values of photocurrent as seen in Fig.6a. To clarify the dynamic response to the used UV illumination, the sample is exposed to UV light [On (light)/ Off (dark)] cycles as shows in Fig. 6a. The sample behavior is recorded directly by using (BK precision Test Bench® 390A multimeter) connected to the PC. The change in the sample photocurrent with exposure time (50 seconds) at constant bias voltage (30 volts) is recorded. The curves demonstrate gradual increase of photocurrent until it attains steady state after 50 seconds. The observed photocurrent steady state indicates the equilibrium between generation and recombination of electron and holes due to fixation of wavelength and intensity of incident UV radiation.

After 50 sec. of attaining steady state photocurrent, the UV lamp power is turned off then the current decay is traced as shows in Fig.6b. The salient feature of On / Off plot is the symmetry of photocurrent rise and decay which suggests that the energy gap is nearly empty from the localized intermediate states which impede the electron/ hole the recombination process.

The sample response to UV illumination could be functionalized by constructing a simple device for ease discrimination between silica, fused silica glass lumps and normal glass lumps.

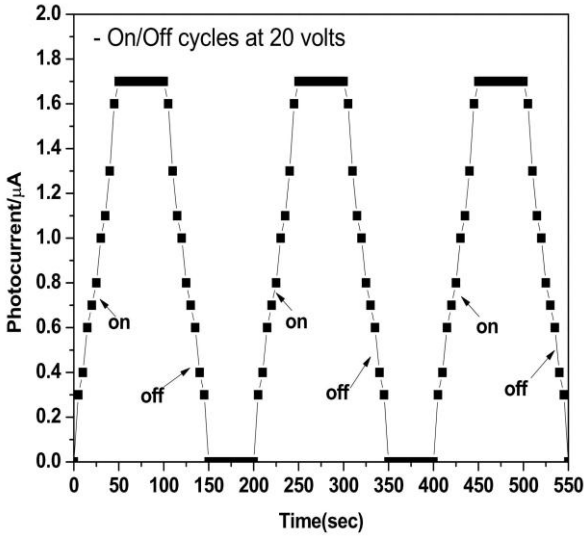

Fig. 6a. The recorded photocurrent response (On/Off cycles) for TiO_2 measured at 20 volts.

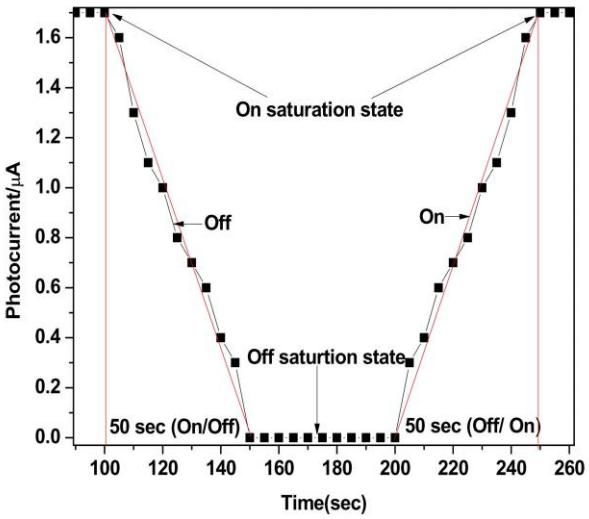

Fig. 6b. The photocurrent response (Off/On cycle).

International Journal of Engineering Research & Technology (IJERT)
ISSN: 2278-0181
Vol. 6 Issue 03, March-2017

IV. CONCLUSIONS

Developed pulse- spray pyrolysis system is used to prepare titanium dioxide films on glass substrates with different thicknesses. The deposited TiO_2 samples are investigated by XRD to elucidate their structure, present phases, particle size, internal strain and dislocation density. Specular transmittance and reflectance of the samples are measured by double beam spectrophotometer via bare glass substrate and Al mirror as a reference, the obtained spectra show interference fringes regardless the sample thickness. Refractive index and film thickness are calculated from the obtained spectra using the method given by Swanepoel. The samples show sharp absorption edge which shifts to the long wavelength for thicker samples. The calculated energy gap from Tauc's plots is found to be 3.35 eV and 3.65 eV for thicker and thinned samples respectively. The samples show high transmittance >85%, low refractive index 2.03 and 19% porosity. A simple setup is designed to measure the photocurrent of the samples when exposed to UV illumination. Static response is performed by exposing the samples to constant UV light and varied biased voltage and measuring the photocurrent.

To clarify the nature of generation/ recombination process dynamic response is carried out at constant bias voltage and UV illumination while the UV lamp power switched on/ off modes during fixed time period. The samples with low thickness give higher photocurrent and linear response. The energy gap of the samples is, to great extent, empty from inter-band states as inferred from the transmittance spectra and dynamic response to UV illumination.

REFERENCES

[1] Barsan, N., D. Koziej, and U. Weimar, Metal oxide-based gas sensor research: How to? Sensors and Actuators B: Chemical, 2007. 121(1): p. 18-35.

[2] Chow, L., et al., Reactive sputtered TiO_2 thin film humidity sensor with negative substrate bias. Sensors and Actuators B: Chemical, 2001. 76(1): p. 310-315.

[3] Selman, A.M. and Z. Hassan, Highly sensitive fast-response UV photodiode fabricated from rutile TiO_2 nanorod array on silicon substrate. Sensors and Actuators A: Physical, 2015. 221: p. 15-21.

[4] Shailesh, P., et al., Fabrication of nanocrystalline TiO_2 thin film ammonia vapor sensor. Journal of sensor technology, 2011. 1(1): p. 9-16.

[5] Xie, T., et al., UV-assisted room-temperature chemiresistive NO_2 sensor based on TiO_2 thin film. Journal of alloys and compounds, 2015. 653: p. 255-259.

[6] Zhang, Y., et al., Synthesis and characterization of TiO_2 nanotubes for humidity sensing. Applied Surface Science, 2008. 254(17): p. 5545-5547.

[7] Bennett, J.M., et al., Comparison of the properties of titanium dioxide films prepared by various techniques. Applied optics, 1989. 28(16): p. 3303-3317.

[8] Karunagaran, B., et al., Structural, optical and Raman scattering studies on DC magnetron sputtered titanium dioxide thin films. Solar energy materials and solar cells, 2005. 88(2): p. 199-208.

[9] Habibi, M.H., N. Talebian, and J.-H. Choi, The effect of annealing on photocatalytic properties of nanostructured titanium dioxide thin films. Dyes and pigments, 2007. 73(1): p. 103-110.

[10] Sarra-Bournet, C., C. Charles, and R. Boswell, Low temperature growth of nanocrystalline TiO_2 films with Ar/O_2 low-field helicon plasma. Surface and Coatings Technology, 2011. 205(15): p. 3939-3946.

[11] Cao, C., et al., UV sensor based on TiO_2 nanorod arrays on FTO thin film. Sensors and Actuators B: Chemical, 2011. 156(1): p. 114-119.

[12] Fujishima, A., K. Hashimoto, and T. Watanabe, TiO_2 photocatalysis: fundamentals and applications. 1999: BKC Incorporated.

[13] Kar, J., et al., Fabrication of UV detectors based on ZnO nanowires using silicon microchannel. Journal of Crystal Growth, 2009. 311(12): p. 3305-3309.

[14] Lee, W.-J. and M.-H. Hon, An ultraviolet photo-detector based on TiO_2/water solid-liquid heterojunction. Applied Physics Letters, 2011. 99(25): p. 251102.

[15] Xue, H., et al., TiO_2 based metal-semiconductor-metal ultraviolet photodetectors. Applied physics letters, 2007. 90(20): p. 201118.

[16] Zhang, D., et al., Enhanced performance of a TiO_2 ultraviolet detector modified with graphene oxide. RSC Advances, 2015. 5(102): p. 83795-83800.

[17] Brevet, A., F. Fabreguette, and L. Imhoff, M. cC. Marco de Lucas, O. Heints, L. Saviot, M. Sacilotti and S. Bourgeois. Surfaces and Coatings Technol, 2002. 151(152): p. 36.

[18] Oja, I., et al. Properties of TiO_2 films prepared by the spray pyrolysis method. in Solid State Phenomena. 2004. Trans Tech Publ.

[19] Syarif, D.G., et al., Preparation of anatase and rutile thin films by controlling oxygen partial pressure. Applied surface science, 2002. 193(1): p. 287-292.

[20] Yu, J., X. Zhao, and Q. Zhao, Effect of surface structure on photocatalytic activity of TiO_2 thin films prepared by sol-gel method. Thin solid films, 2000. 379(1): p. 7-14.

[21] Obaida, M., I. Moussa, and M. Boshta, Low Sheet Resistance F-Doped SnO_2 Thin Films Deposited by Novel Spray Pyrolysis Technique. International Journal of ChemTech Research, 2015. Vol.8(No.12): p. pp 239-247.

[22] Ba-Abbad, M.M., et al., Synthesis and catalytic activity of TiO_2 nanoparticles for photochemical oxidation of concentrated chlorophenols under direct solar radiation. Int. J. Electrochem. Sci, 2012. 7: p. 4871-4888.

[23] Bagheri, S., K. Shameli, and S.B. Abd Hamid, Synthesis and characterization of anatase titanium dioxide nanoparticles using egg white solution via Sol-Gel method. Journal of Chemistry, 2012. Vol. 2013.

[24] Dhanapandian, S., A. Arunachalam, and C. Manoharan, Effect of deposition parameters on the properties of TiO_2 thin films prepared by spray pyrolysis. Journal of Sol-Gel Science and Technology, 2016. 77(1): p. 119-135.

[25] Ranganayaki, T., et al., Preparation and characterization of nanocrystalline TiO_2 thin films prepared by sol–gel spin-coating method. J. Innovative Res. Sci, 2014. 3(10): p. 16707-16713.

[26] Williamson, G. and W. Hall, X-ray line broadening from filed aluminium and wolfram. Acta metallurgica, 1953. 1(1): p. 22-31.

[27] Kose, S., et al., In doped CdO films: electrical, optical, structural and surface properties. International journal of hydrogen energy, 2009. 34(12): p. 5260-5266.

[28] Swanepoel, R., Determination of the thickness and optical constants of amorphous silicon. Journal of Physics E: Scientific Instruments, 1983. 16(12): p. 1214.

[29] Tauc, J., R. Grigorovici, and A. Vancu, Optical properties and electronic structure of amorphous germanium. physica status solidi (b), 1966. 15(2): p. 627-637.

[30] Mezza, P., J. Phalippou, and R. Sempere, Sol–gel derived porous silica films. Journal of non-crystalline solids, 1999. 243(1): p. 75-79.